Eur. J. Biochem. **264**, 1–12 (1999) © FEBS 1999

Characterization of the ternary complex between Rab7, REP-1 and Rab geranylgeranyl transferase

Kirill Alexandrov, Iris Simon*, Vyacheslav Yurchenko†, Andrei Iakovenko, Elena Rostkova, Axel J. Scheidig and Roger S. Goody

Department of Physical Biochemistry, Max-Planck Institute for Molecular Physiology, Dortmund, Germany

Geranylgeranylation is a post-translational modification of Rab GTPases that enables them to associate reversibly with intracellular membranes. Geranylgeranylation of Rab proteins is critical for their activity in controlling intracellular membrane transport. According to the currently accepted model for their action, newly synthesized Rab proteins are recruited by Rab escort protein (REP) and are presented to the Rab geranylgeranyl transferase (RabGGTase) which covalentely modifies the Rab protein with two geranylgeranyl moieties. After prenylation, the Rab protein remains in complex with REP and is delivered to the target membrane by the latter. In this work, we show that RabGGTase can form a stable complex with Rab7–REP in the absence of its lipid substrate geranylgeranyl pyrophosphate. In order to characterize this interaction, we developed three fluorescence assays reporting on the interaction of RabGGTase with the Rab7–REP complex. For this interaction we determined a K_d value of about 120 nM.

Association of RabGGTase with the Rab7–REP complex occurs with a rate constant of $\approx 10^8$ $M^{-1} \cdot s^{-1}$. We demonstrate that the state of the nucleotide bound to Rab7 does not influence the affinity of RabGGTase for the Rab7–REP-1 complex. Finally, we address the issue of substrate specificity of RabGGTase. Titration experiments demonstrate that, in contrast with farnesyl transferase, RabGGTase does not recognize a defined C-terminal sequence motif. Experiments using Rab7 mutants in which the last 16 amino acids were either mutated or truncated revealed that the distal part of the C-terminus makes only a limited contribution to the binding affinity between RabGGTase and the Rab7–REP-1 complex. This demonstrates the functional dissimilarity between RabGGTase and geranylgeranyl transferase I and farnesyl transferase, which interact specifically with the C-terminus of their substrates. Based on these experiments, we propose that RabGGTase recognizes the overall structure arising from the association of Rab and REP and then 'scans' the flexible C-terminus to position the proximal cysteines into the active site.

Keywords: geranylgeranylation; prenyltransferase; Rab7; Rab geranylgeranyl transferase; REP.

Rab proteins are members of the Ras superfamily of small GTP-binding proteins. Many of them were shown to be implicated in control of intracellular vesicular traffic [1,2]. For their function Rab proteins require modification by geranylgeranyl isoprenoids. This allows them to associate reversibly with a membrane in a tightly controlled fashion [3,4]. Covalent attachment of geranylgeranyl groups to two C-terminal cysteines is catalyzed by Rab geranylgeranyl transferase (RabGGTase).

Correspondence to R. S. Goody, Department of Physical Biochemistry, Max-Planck Institute for Molecular Physiology, Otto-Hahn-Strasse 11, 44227 Dortmund, Germany. Telefax: + 49 0231 1331651, Tel.: + 49 0231 1332300, E-mail: goody@mpi-dortmund.mpg.de

Abbreviations: GGpp, geranylgeranyl pyrophosphate; Rab, Ras-like protein from rat brain; RabGGTase, Rab geranylgeranyl transferase; REP, Rab escort protein; mant, *N*-methylanthraniloyl; FRET, fluorescence resonance energy transfer; 1,5-IAEDANS, 5-({[(2-iodoacetyl)amino]ethyl}amino)-naphthalene-1-sulfonic acid; 5-TMRIA, tetramethylrhodamine-5-iodoacetamide dihydroiodide; TEV, tobacco etch potyvirus.

**Present address*: Department of Biochemistry, Stanford University School of Medicine, Stanford, CA 94305-5307, USA.

†*Present address*: Department of Molecular Biology, Moscow State University, Moscow 119899, Russia.

(Received 21 April 1999; revised 21 June 1999; accepted 7 July 1999)

Mammalian RabGGTase (GGTase II) is a heterodimer composed of tightly associated α and β subunits of 60 and 38 kDa, respectively [5,6], and belongs to the family of protein prenyl transferases together with farnesyl transferase and geranylgeranyl transferase I (GGTase I) [7]. Substrates of farnesyl transferase include members of the Ras family, lamin β and several other proteins. GGTase I prenylates γ subunits of heterotrimeric G-proteins as well as members of the Ras, Rac and Rho families [7]. A distinct feature of farnesyl transferase and GGTase I is their ability to recognize a short C-terminal motif often referred to as the CAAX box (C, cysteine; A, aliphatic; X, serine/methionine/alanine) which is subjected to post-translational modification by isoprenoids. The choice between farnesylation and geranylgeranylation is determined by the hydrophobicity of the X residue [7]. Original studies suggested that the prenylation reaction catalyzed by farnesyl transferase or GGTase I proceeds via a random sequential mechanism by which the enzyme can bind the protein and lipid substrates independently [8,9]. However, recent studies with human and yeast farnesyl transferase supported an ordered addition of substrates [10,11].

In contrast with other known prenyl transferases, RabGGTase does not recognize its substrate directly but exerts its function in concert with another protein termed REP (Rab escort protein) [12,13]. Two known mammalian proteins,

REP-1 and REP-2, share 75% amino acid sequence identity and functionally overlap [14]. Both of them have several stretches of high sequence homology to Rab-GDP dissociation inhibitor, a cytosolic factor responsible for delivery and removal of Rab proteins to and from the membrane [3,4,15]. According to the current model, a newly synthesized Rab protein forms a stable complex with REP [7,16]. RabGGTase recognizes the Rab–REP complex and covalentely attaches the geranylgeranyl group to two C-terminal cysteines of the Rab protein [13,17]. RabGGTase is able to prenylate cysteines in a much broader context of amino acids than farnesyl transferase or GGTase I making it impossible to derive a definitive C-terminal consensus sequence [7]. It was demonstrated that mutation of the C-terminal sequence CC of Rab1a to CSC did not affect the prenylation efficiency [18]. It is also worth noting that, although the majority of Rab proteins possess two prenylatable cysteines at the C-terminus, there are several exceptions. Rab8, Rab13, Rab18, Rab 23 and Rab 28 possess only one C-terminal cysteine in the amino acid context similar to that of Ras and Rho proteins. Rab8 and Rab11 were shown to undergo geranylgeranylation *in vitro* [19]. A recent detailed study revealed that, although Rab8 can be efficiently prenylated by both GGTase I and RabGGTase *in vitro,* the majority of the protein was prenylated by RabGGTase *in vivo*. This study suggests that, for Rab protein recognition, RabGGTase needs motifs other than the C-terminus [20].

An earlier study suggested that prenylation is brought about by transient association of RabGGTase with the Rab–REP complex [13]. This report suggested that there is no strict order of addition of the isoprenoid to the acceptor residues although the cysteine second from the end is preferred. It has also been suggested that RabGGTase processes preferentially monoprenylated Rab proteins thus driving the reaction towards the doubly modified product [21]. However, the exact sequence of events as well as the kinetic mechanism of the prenylation reaction remains largely unexplored. After prenylation, the Rab protein remains bound to REP which accompanies it to the corresponding membrane [12,22]. The Rab protein is released on to the membrane, presumably through interaction with a membrane receptor/REP-displacing factor which might be shared by REP and GDP-dissociation inhibitors [23]. As a result, REP is released into the cytosol and can enter a new prenylation cycle. Although the prenylation reaction has been reconstituted *in vitro* [13,24], only limited data are available on the interaction of its components at the molecular level. In the current study we have analyzed the interactions between Rab7, REP-1 and RabGGTase using solid-phase precipitation assays, gel-filtration chromatography and fluorescent spectroscopy. We present evidence that RabGGTase can bind its protein substrate tightly in the absence of lipid. We characterize this interaction and demonstrate that the C-terminus of Rab7 plays only a minor role in protein substrate recognition by RabGGTase.

EXPERIMENTAL PROCEDURES

Expression vectors

Construction of a pET19b-TEV expression plasmid. A pTL-5495 plasmid containing a genomic fragment with the coding sequence of tobacco etch potyvirus protease (TEV protease) was obtained from the American Type Cell Collection (accession number 45036). The coding sequence of TEV protease was amplified by PCR using Expand polymerase (Boehringer-Mannheim) with the following primers containing *Xho*I and *Bam*HI sites: 5′-GGTGACTCGAGGGAGAA-AGCTTGTTTAAG-3′ and 5′-CTCAGGATCCCTATCATTGC-GAGTACACCAATTC-3′. PCR product was gel purified, digested with *Xho*I and *Bam*HI restriction enzymes and ligated into the pET-19b expression vector (Novagen). The integrity of the reading frame and the coding sequence was determined by nucleotide sequencing.

Construction of pHT-Rab7 expression vector and C-terminal mutants of Rab7. To generate the pHT-Rab7 vector, the Rab7 coding sequence was excised from pET3-Rab7 [25] vector using *Nde*I and *Xho*I sites and subcloned into the pHT expression vector in-frame with an N-terminal histidine tag and TEV protease cleavage site. The final plasmid was analyzed by restriction digestion and DNA sequencing. Mutations in the C-terminal region of Rab7 were introduced by PCR using 1 ng of the original pHT-Rab7 clone. The list of primers is available from the authors on request. The presence of mutations and integrity of the coding sequence were verified by DNA sequencing.

Expression and purification of TEV protease

Expression and purification of TEV protease was performed as described previously [26]. TEV protease was concentrated with a Centriprep 10 concentrator (Amicon), shock-frozen and stored in multiple aliquots at −80 °C.

Expression and purification of wild-type and mutants of Rab7. The plasmids were transformed into *Escherichia coli* BL21(DE3) strain and cells were grown and induced with isopropyl β-D-thiogalactoside as described previously [27]. His-tagged wild-type Rab7 and Rab7 mutants were purified on 1 mL Hi-Trap Ni–agarose columns (Pharmacia) by Ni-affinity chromatography according to the instructions of the manufacturer. Eluates were analyzed by SDS/PAGE followed by Coomassie blue staining. Fractions containing Rab7 were pooled, and protein was precipitated by the addition of ammonium sulfate to 75% and pelleted by centrifugation at 21 000 ***g*** for 15 min. The supernatant was discarded and the protein pellet was resuspended in 5 mL 25 mM Na_2HPO_4, pH 8.0, containing 5 mM 2-mercapthoethanol. TEV protease was added to the sample at a 1 : 100 molar ratio. The reaction mixture was incubated at room temperature for 1 h. Progression of the reaction was determined by SDS/PAGE, and typically at the end of the incubation over 85% of the protein was cleaved. The sample was passed over a 1-mL Ni–agarose column (Pharmacia) pre-equilibrated with 50 mM Na_2HPO_4, pH 8.0, containing 0.3 M NaCl and 2 mM 2-mercapthoethanol in order to remove the polyhistidine tags, uncleaved protein, TEV protease and impurities. The column was subsequently washed with 5 mL of the equilibration buffer. The specificity of the TEV protease digestion of wild-type His–TEV–Rab7 fusion protein was confirmed by N-terminal protein sequencing. Further purification was performed on a Superdex 75 16/60 gel-filtration column pre-equilibrated with buffer consisting of 50 mM Hepes, pH 7.2, 50 mM NaCl, 2 mM $MgCl_2$, 5 mM dithioerythritol and 100 μM GDP. Fractions of volume 4 mL were collected and analyzed by SDS/PAGE followed by Coomassie blue staining. Fractions containing pure protein were pooled, concentrated using Centripreps 10 (Amicon) and stored in multiple aliquots at −80 °C. Typical protein purity was over 95% as judged by Coomassie blue staining and MS.

Expression and purification of REP-1 and RabGGTase

REP-1 was expressed and purified essentially as described elsewhere with slight modifications [14]. Briefly, Sf21 cells were infected with recombinant baculovirus encoding REP-1, grown, lysed by sonication and the 100 000 ***g*** supernatant was subjected to Ni–Sepharose affinity chromatography as described above for the His-tagged Rab7 proteins. The His-tagged REP-1 was dialyzed against a buffer containing 25 mM Hepes, pH 7.2, 10 mM NaCl and 2 mM 2-mercapthoethanol and concentrated using Centripreps 30 (Amicon). Further purification was performed on a Superdex 200 16/60 gel-filtration column (Pharmacia) pre-equilibrated with 25 mM Hepes, pH 7.2, containing 20 mM NaCl and 5 mM dithioerythritol. Fractions of volume 4 mL were collected and analyzed by SDS/PAGE followed by Coomassie blue staining. Fractions containing pure REP-1 were pooled and concentrated using Centripreps 30 (Amicon). Protein was more then 95% pure as judged by SDS/PAGE and stored in multiple aliquots at −80 °C. For expression of RabGGTase, baculoviral expression vectors pVL-RabGGTalpha and pVL-RabGGTbeta were obtained from the American Type Culture Collection (accession numbers 87154 and 87155, respectively). Baculoviruses were generated and RabGGTase was expressed and purified essentially as described previously [28]. Briefly, Sf21 cells were co-infected with recombinant baculovirus encoding the α and the β subunit, grown, and collected by centrifugation. Cells were lysed by sonication on ice in 50 mM Hepes, Q2 pH 7.2, containing 10 mM NaCl, 2 mM BME, 1 mM phenylmethanesulfonyl fluoride, 1 mM 2-mercaptoethanol, 5 $\mu g \cdot mL^{-1}$ pepstatin, 5 $\mu g \cdot mL^{-1}$ leupeptin and 5 $\mu g \cdot mL^{-1}$ aprotinin, and a 100 000 ***g*** supernatant was prepared. The supernatant was chromatographed on a 20-mL Poros HQ Q3 column (PerSeptive Biosystems) equilibrated with 50 mM Hepes, pH 7.2, containing 10 mM NaCl and 2 mM BME. Proteins were resolved by an NaCl gradient 10–500 mM. Fractions containing RabGGTase were collected and $(NH_4)_2SO_4$ was added to 300 mM. A sample was then loaded on to a 15-mL phenyl-Sepharose (Pharmacia) column equilibrated with buffer consisting of 25 mM Tris/HCl, pH 8.0, 300 mM $(NH_4)_2SO_4$ and 2 mM BME. Protein was eluted with a linear gradient (300–5 mM) of $(NH_4)_2SO_4$, and fractions containing RabGGTase were precipitated with 75% $(NH_4)_2SO_4$. Protein was pelleted, resuspended in 5 mL of 50 mM Hepes, pH 7.2, containing 10 mM NaCl and 2 mM BME and loaded on to the Superdex 200 column (Pharmacia) equilibrated with the same buffer. Fractions containing RabGGTase were pooled and concentrated. The protein was more then 90% pure as judged by SDS/PAGE and stored in multiple aliquots at −80 °C.

Determination of geranylgeranyl pyrophosphate (GGpp)-bound state of RabGGTase

RabGGTase (10 nmol) was incubated with 60 units of alkaline phosphatase (Sigma) in 300 μl of buffer containing 50 mM Tris/HCl, pH 8.0, 10 mM NaCl and 2 mM dithioerythritol at room temperature for 1 h. The sample was then loaded on to a Micron 30 concentrator (Amicon) concentrated to 30 μl, and the flow-through collected. The concentrate was diluted once again with the reaction buffer and concentrated by the same procedure. The combined flow-through (550 μL) was mixed with 200 mL chloroform and vortex-mixed. The chloroform phase was collected and the sample re-extracted with the same volume of chloroform. The combined chloroform extract was evaporated and 30 μl 25 mM NH_4OH added. The presence of geranylgeranyl alcohol was determined by electrospray ionization MS using an LCQ mass spectrometer (Finnigan). In the Q4 control experiments, RabGGTase was replaced with 10 nmol of GGpp, processed and analyzed as above.

To estimate the amount of GGpp bound to recombinant RabGGTase after purification from baculovirus-infected insect cells or upon loading with GGpp, we took advantage of the ability of butan-1-ol to extract phosphoisoprenoids from aqueous solutions. Routinely we extracted 10 nmol of RabGGTase, RabGGTase–GGpp complex or GGpp with butan-1-ol. After evaporation of the butanol, pellets were resuspended in 100 mM Tris/HCl buffer, pH 8.3 supplemented with 1 mM $MgCl_2$ and 100 μM $ZnCl_2$, and 4 U alkaline phosphatase added to each sample. Geranylgeranyl alcohol generated was extracted with hexane, concentrated by evaporation and spotted on to TLC RP-18 plates along with prenyl alcohol standards. Samples were developed with an acetone/water mixture (9 : 1, v/v) and visualized using iodine vapor.

Electrospray ionization MS

Electrospray ionization MS measurements were carried out using am LCQ MS instrument in the positive ion mode. In the case of proteins 1 μL protein solution was mixed with 9 μL 50% formic acid/5% methanol, and 3 μL was used for injection. For geranylgeranyl alcohol, samples were diluted 1 : 9 with acetonitrile before injection. Measurements and analysis were performed according to the instructions of the manufacturer.

Nucleotides and nucleotide exchange

N-Methylanthraniloyl derivatives (mant) of GDP and GTP were prepared as described previously [29]. The mantGDP- and mantGTP-bound forms of Rab7 were prepared as described previously [27]. Efficiency of the nucleotide exchange was confirmed by HPLC on a C_{18} reversed-phase column using a Beckman Gold HPLC system calibrated with standard solutions of mGDP and mGTP under the conditions described previously. Typically exchange efficiency was over 90%. The GTP form of Rab7 was prepared as described previously [27], and exchange efficiency was analyzed by HPLC as described in the following section. Exchange efficiency was typically over 90%.

GTPase assay

GTP hydrolysis was assayed as a function of time by HPLC on a C_{18} reversed-phase column in the presence of tetrabutylammonium bromide under isocratic conditions [30]. The reaction mixture contained 5 μM Rab7GTP, 5 μM REP-1 and 25 μM RabGGTase in 180 μL of the 25 mM Hepes (pH 7.2)/20 mM NaCl/5 mM dithioerythritol buffer. The reaction mixture was incubated at 37 °C and a 20 μL sample was injected on the column every 30 min.

Labeling of Rab7 with 5-({[(2-iodoacetyl)amino]ethyl}amino) naphthalene-1-sulfonic acid (1,5-IAEDANS)

Wild-type or mutant Rab7 (50 nmol) was incubated with 1 μmol 1,5-IAEDANS (Molecular Probes) in 300 μL of 100 mM Tris/HCl, pH 8.0, for 2 h at 4 °C. After the incubation period, the protein was passed through two 3 mL Sephadex G-25 (Pharmacia) spin columns pre-equilibrated with 20 mM

Hepes, 7.2, containing 10 mM NaCl and 2 mM dithioerythritol. Labeled protein was stored in multiple aliquots at −80 °C.

Labeling of Rab7 with tetramethylrhodamine-5-iodoacetamide dihydroiodide (TMRIA)

Rab7 (50 nmol) was incubated with 1 μmol TMRIA for 12 h at 4 °C in buffer (50 mM Tris/HCl, pH 8.0, 50 mM NaCl, 2 mM dithioerythritol, 10 μM GDP). Protein was separated from the unreacted dye on a PD-10 column (Pharmacia) equilibrated with buffer (50 mM Tris/HCl, pH 8.0, 50 mM NaCl, 2 mM dithioerythritol). Unlabeled Rab7 was separated by chromatography on a 1-mL Poros HQ anion-exchange column equilibrated with buffer (50 mM Tris/HCl, pH 8.0, 10 mM NaCl, 2 mM dithioerythritol, 10 μM GDP). Protein was eluted with a salt gradient from 10 to 500 mM NaCl. Labeled protein was eluted in two peaks at about 90–150 mM and 250 mM NaCl. It was dialyzed against 20 mM Hepes, 7.2, containing 10 mM NaCl, 2 mM dithioerythritol and 10 μM GDP, and aliquots were stored frozen at −80 °C.

Fluorescence measurements

Fluorescence spectra and long-time-base fluorescence measurements were performed with an Aminco SLM 8100 spectrophotometer (Aminco, Silver Spring, MD, USA). All reactions were followed at 25 °C in 25 mM Hepes, pH 7.2, containing 40 mM NaCl, 2 mM $MgCl_2$ and 2 mM dithioerythritol. Fluorescence of mantGDP and dansyl-labeled Rab7 were excited via fluorescence resonance energy transfer (FRET) from tryptophan at 295 nm and measured at 440 nm. For the measurement of the direct fluorescence signal, dansyl-labeled Rab7 was excited at 333 nm and data were collected at 440 nm. For the measurement of the direct fluorescence signal, the rhodamine-labeled Rab7 was excited at 570 nm and data were collected at 590 nm. Stopped-flow experiments using dansyl-labeled Rab7 were performed in a High-Tech Scientific SF61 apparatus (Salisbury, Wilts., UK). The dansyl fluorescence was excited at 290 or 333 nm and detected through a 389-nm cut-off filter. Data collection and primary analysis of rate constants were performed with the package from High Tech Scientific, the secondary analysis was performed with the programs GRAFIT 3.0 (Erithacus software) and SCIENTIST 2.0 (MicroMath Scientific Software).

Analytical gel-filtration chromatography

Protein complex formation was performed in 150 μL 40 mM Hepes, pH 7.2, containing 150 mM NaCl, 5 mM dithioerythritol and 3 mM $MgCl_2$. Depending on the experiment, the 100 μL reaction mixture contained 5 μM REP-1, 15 μM RabGGTase or 11 μM Rab7 and 100 μM GGpp. The sample was mixed, centrifuged in a bench top centrifuge for 5 min and loaded on to a Superdex 200 column 10/20 gel-filtration column driven by a Waters 490E HPLC system. The column was calibrated using a gel-filtration calibration kit (Bio-Rad). Flow rate was 0.4 $mL \cdot min^{-1}$. Peaks were collected manually and protein precipitation was performed with 10% trichloroacetic acid. Samples were analyzed by SDS/PAGE followed by Coomassie blue staining.

Ni–agarose precipitation assay

Ni–agarose beads (30 μL; Qiagen) were prewashed with 40 mM Hepes, pH 7.2, containing 20 mM NaCl, 1 mM BME, 1 mM $MgCl_2$, 100 μM GDP, 0.5% glycerol and 0.005% Triton X-100, and incubated with 100 pmol REP-1, RabGGTase or 200 pmol Rab7 in different combinations for 20 min at 4 °C. After incubation, the beads were washed four times with the same buffer and 30 μL Laemmli buffer was added. Samples were analyzed by SDS/PAGE followed by Coomassie blue staining.

RESULTS

Detection of Rab7–REP-1–RabGGTase complex by solid-phase precipitation assays

In the work presented here, we sought to explore the interaction between RabGGTase and its protein substrate Rab7. We first analyzed the interaction of RabGGTase with Rab7 and REP-1 employing solid-phase precipitation assays. We took advantage of the fact that REP-1 contained a His_6 tag on its N-terminus and thus could be precipitated with Ni–agarose beads. In our experiment, we incubated different combinations of proteins with Ni–agarose beads for 20 min at 4 °C and after extensive washing eluted bound proteins by boiling with Laemmli buffer. Samples were resolved by SDS/PAGE (15% gel). As shown in Fig. 1, RabGGTase was recovered on the beads together with REP-1 and Rab7. Binding of RabGGTase was dependent on the presence of the Rab7–REP-1 complex and no binding was observed with Ni–agarose beads alone (Fig. 1).

Stoichiometry of the ternary complex

To determine the stoichiometry of the ternary complex we employed analytical gel filtration on a Superdex 200 column. First, we determined the retention time of each protein separately. Rab7, REP-1 and RabGGTase were eluted with retention times corresponding to 22, 90 and 86 kDa, respectively (data not shown). This indicates that, under the chosen conditions, all three proteins are present in the solution as monomers. Next we injected on to the column mixtures of Rab7 with RabGGTase or REP-1 with RabGGTase. In both cases proteins were eluted from the column at their monomeric positions (data not shown). When REP-1 was preincubated with an excess of Rab7, two peaks of about 130 and 22 kDa were recovered (Fig. 2A). As revealed by SDS/PAGE, the 130-kDa

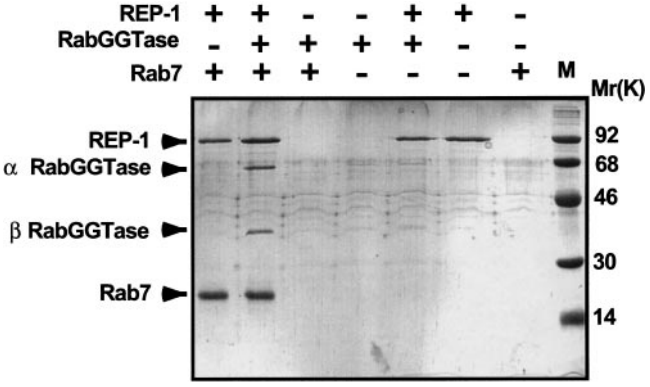

Fig. 1. Detection of the ternary Rab7–REP-1–RabGGTase complex by Ni–Sepharose affinity precipitation. Rab7, RabGGTase and His-REP-1 were incubated with Ni–Sepharose in different combinations as indicated and described in Experimental Procedures. After incubation, the samples were washed with the incubation buffer and aliquots of the pellet analyzed by SDS/PAGE. Molecular mass is indicated on the right in kDa.

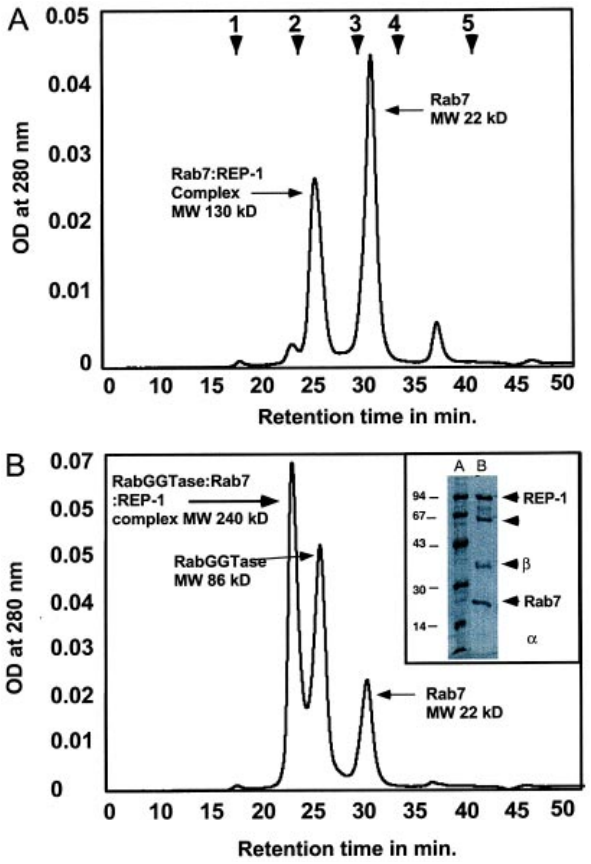

Fig. 2. Detection of the Rab7–REP-1–RabGGTase complex by gel-filtration chromatography. Each reaction mixture contained in a final volume of 100 μL, 11 μM Rab7, 5 μM REP-1 (A), 11 μM Rab7, 5 μM REP-1, 15 μM RabGGTase (B) or 11 μM Rab7, 5 μM REP-1, 15 μM RabGGTase, 100μM GGpp (C). After incubation each sample was loaded on to a Superdex 200 10/20 column equilibrated and run at a flow rate of 0.4 mL·min^{-1} as described in Experimental Procedures. The molecular mass (MW) of the peaks was determined by comparison with protein standards of known molecular mass (1, 670 kDa; 2, 158 kDa; 3, 44 kDa; 4, 17 kDa; 5, 1.3 kDa; shown as arrowheads in A). Manually collected peaks were precipitated with trichloroacetic acid, subjected to SDS/PAGE on 15% mini gels, and the proteins visualized by Coomassie blue staining. The inset of (B) shows the protein composition of the 240-kDa peak in the lane B compared with a molecular-mass standard in lane A. Horizontal arrows indicate the position of migration of REP, α and β subunits of RabGGTase and Rab7 (right), and the molecular-mass markers (left). OD, Absorbance.

peak contained REP-1 and Rab7 in a 1 : 1 ratio as judged from the intensity of the Coomassie-stained bands (data not shown). This corresponds well to previous observations [12,13,31]. In the following experiment we supplemented the same reaction mixture with a twofold molar excess of RabGGTase over REP-1. As depicted in Fig. 2B, in this case the major peak was detected at the position corresponding to 240 kDa in addition to two smaller peaks at 87 and 22 kDa. SDS/PAGE analysis revealed that the 240-kDa peak contained REP-1, Rab7 and RabGGTase in the proportions 1 : 1 : 1 (inset of Fig. 2B). The second and third peaks contained free RabGGTase and Rab7, respectively. This experiment suggested that REP-1, Rab7 and RabGGTase can form a stable ternary complex in the absence of lipid substrate. However, it is possible that the RabGGTase has GGpp bound that was carried through the enzyme purification as has been reported for farnesyl transferase [32]. In this case bound GGpp could contribute to the binding of

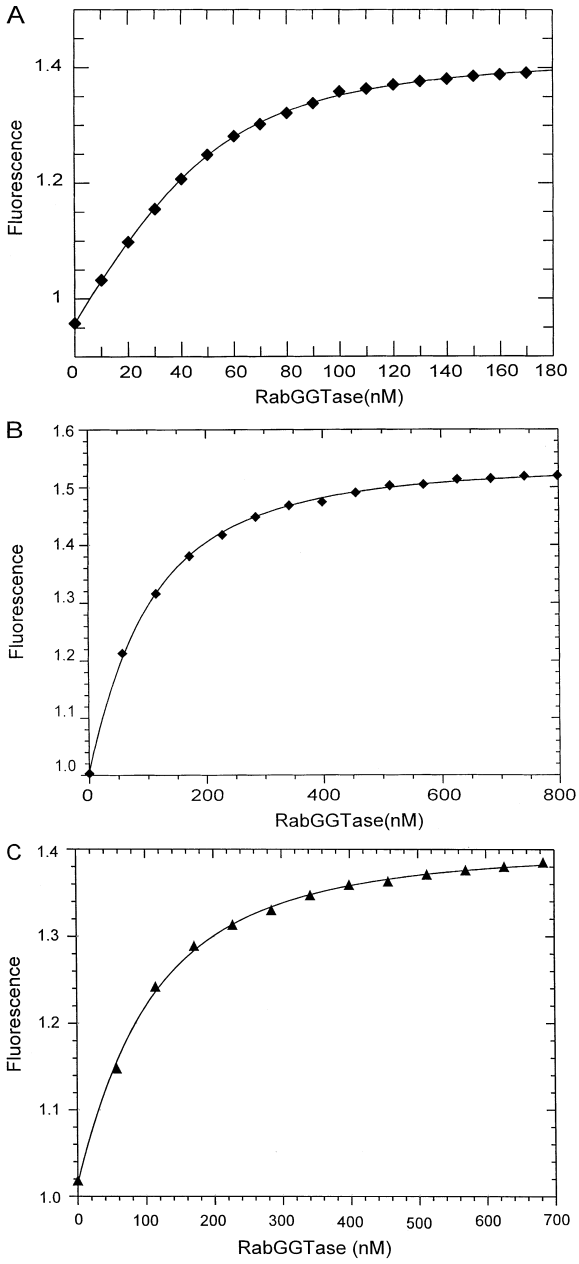

Fig. 3. Spectrofluorimetric titration of dansyl-Rab7–REP-1 complex with RabGGTase. (A) Conditions: 25 °C, 25 mM Hepes, pH 7.2, 40 mM NaCl, 2 mM $MgCl_2$ and 2 mM dithioerythritol. The concentration of Rab7–REP-1 complex was 50 nM. The excitation/emission wavelengths were fixed at 333/440 nm. Data were analyzed as described in Experimental procedures. (B) Spectrofluorimetric competition titration of dansyl-Rab7–REP-1 fluorescence by GGpp-free RabGGTase in the presence of Rab7–REP-1 complex. The dansyl-Rab7–REP-1 complex concentration was 50 nM, wild-type Rab7–REP-1500 nM. Data were fitted using the program SCIENTIST 2.0 and gave K_d values of 120 nM for the interaction of RabGGTase with the unlabeled Rab7–REP-1 complex. (C) Result of a spectrofluorimetric competition titration of the dansyl-Rab7–REP-1 fluorescence signal by RabGGTase in the presence of GppNHp–Rab7 complexed to REP-1. The dansyl-Rab7–REP-1 complex concentration was 50 nM, Rab7 (GppNHp)–REP-1–500 nM. Data were fitted using the program SCIENTIST 2.0 The K_d value for the interaction of Rab7 (GppNHp)–REP-1 with RabGGTase was determined to be 121 nM (A).

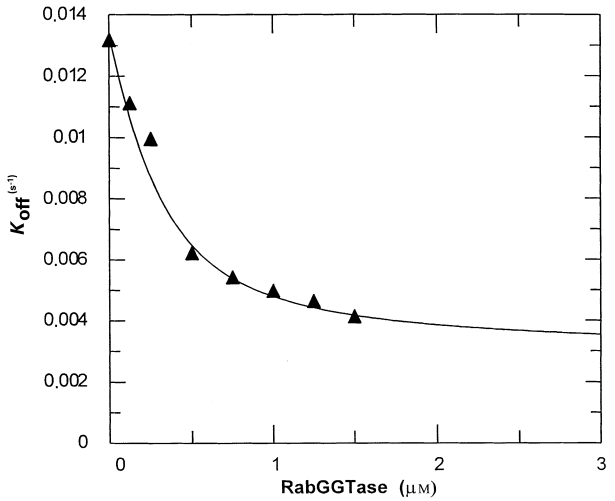

Fig. 4. Effect of RabGGTase on the dissociation rate constant of the Rab7–REP-1 complex. Buffer conditions were as described for Fig. 3. The time course of the energy transfer signal change seen on mixing Rab7(mGDP)–REP-1 (0.25 μM) with Rab7(GDP) (2.5 μM) in the spectrophotometer was followed at different concentrations of added RabGGTase. Excitation was at 289 nm, and emission was detected at 440 nm. The single exponential equation fits of observed rates were plotted against the concentrations of RabGGTase. The data were analyzed as described in the text to give a K_d of 172 nM.

RabGGTase to the Rab protein, or reaction product (prenylated Rab) could be generated. It was therefore necessary to determine the isoprenoid-bound state of RabGGTase using a direct method. RabGGTase was treated with alkaline phosphatase to remove the phosphate as described in Experimental procedures. Geranylgeranyl alcohol was extracted as described and subjected to electrospray MS. A peak of molecular mass 271 Da was observed when either alkaline phosphatase-treated GGpp or the extract of alkaline phosphatase-treated RabGGTase was analyzed. This mass corresponds to the calculated molecular mass of geranylgeranyl alcohol, and was not present in preparations of RabGGTase that were pretreated with alkaline phosphatase and dialyzed. This analysis provides evidence that the lipid removal was complete in this case (data not shown).

To estimate the amount of GGpp bound to recombinant RabGGTase after purification from baculovirus-infected insect cells, we extracted 10 nmol RabGGTase, RabGGTase–GGpp complex or GGpp with butan-1-ol. Samples were treated as described in Experimental Procedures and analyzed by TLC reversed-phase chromatography. Although this method does not allow exact quantification, we could conclude from the intensity of the spots that less then 10% of the RabGGTase was GGpp-bound (data not shown). This finding can be explained by a large amount of phosphatase activity in cellular lysates resulting in deposphorylation of phosphoisoprenoid and dissociation of geranylgeraniol from the RabGGTase (A. Iakovenko *et al.*, unpublished work).

We repeated the gel-filtration experiments described above using GGpp-free RabGGTase. As in the earlier case, a peak of about 240 kDa was recovered in addition to the 89-kDa and 23-kDa peaks (data not shown). Our observations appeared to contradict earlier observations that RabGGTase and the Rab–REP-1 complex migrate separately on gel filtration [12,13]. In these cases, however, experiments were performed with an excess of GGpp and under conditions that allowed prenylation of the substrate. This result suggests that the prenylated product may have lower affinity for the enzyme than the substrate, which explains why the product–enzyme complex is not detectable by gel filtration. Initial experiments indicate that this is the case (K. Alexandrov *et al.*, unpublished work).

Development of fluorescent interaction assays and determination of RabGGTase affinity for the Rab7–REP-1 complex

Having determined the stoichiometry of the Rab7–REP-1–Rab GGTase ternary complex, we wished to devise a method for determining the binding affinity of RabGGTase for the Rab7–REP-1 complex. It is known that the C-terminus of Rab7 does not possess a defined structure in solution [25]. However, logic demands that two C-terminal cysteines must be precisely positioned for a prenyl-transfer reaction catalyzed by RabGGTase. This would obviously require a large structural rearrangement and hence must introduce changes in the environment of the C-terminal cysteines. This rationale motivated us to introduce a fluorescent group into the C-terminal cysteines of Rab7 which could report on interaction with RabGGTase. To ensure the specificity of the proposed labeling, we examined the structure of Rab7 (Metcalf, personal communication). There are five cysteines in the Rab7 structure: C83, C84, C143, C207 and C205. C83 and C84 are situated in the core of the molecule, while C143 is on the hydrophobic side of a helix facing towards the core. Thus, only the C-terminal cysteines C205 and C207 are likely to be labeled when challenged by a water-soluble reagent. With this in mind, we modified Rab7 with dansyl groups using 1,5-IAEDANS as described in Experimental Procedures. Excitation and emission scans of the labeled protein revealed that fluorescence could be excited either directly at 333 nm or via FRET from tryptophan at 295 nm. To estimate the labeling efficiency, we subjected Rab7 and dansyl-Rab7 to nanospray MS and obtained molecular masses of 23388 Da and 24001 Da, respectively (data not

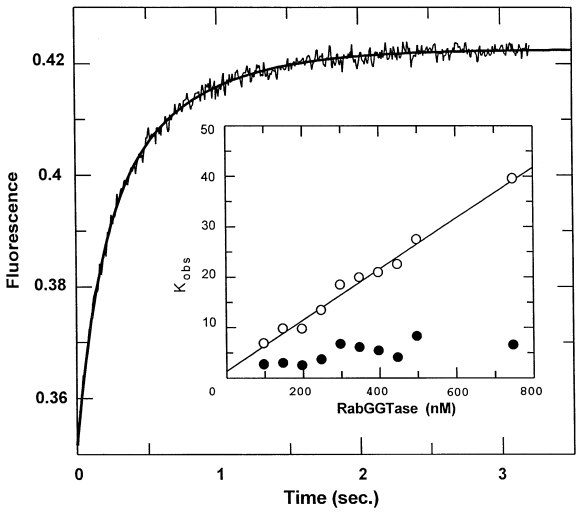

Fig. 5. Time course of the FRET signal change seen on mixing dansyl-Rab7–REP-1 complex (50 nM) with RabGGTase (100 nM) in the stopped-flow apparatus. Excitation was at 289 nm, and emission was detected through a 389-nm cut-off filter. The fit shown is to a double-exponential equation with rate constants of 6.6 s^{-1} (k_{ass1}) and 2.4 s^{-1} (k_{ass2}). The inset shows the secondary plot of data from 10 experiments of the above type. (○) k_{1obs} and (●) k_{2obs} values plotted against the concentration of RabGGTase.

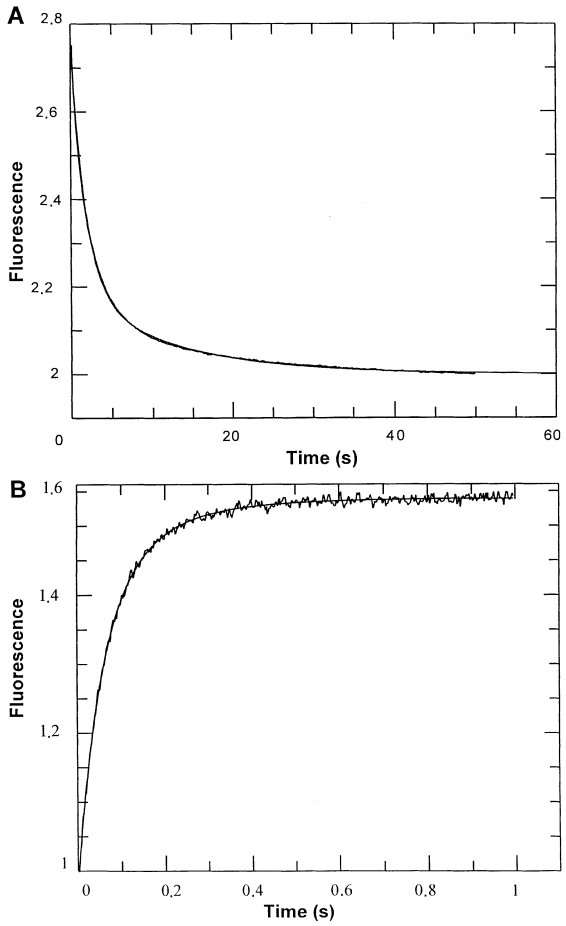

Fig. 6. Time course of the energy-transfer signal change seen upon mixing dansyl-Rab7–REP-1–RabGGTase (0.1 μM) with Rab7–REP-1 (2.0 μM) in the stopped-flow apparatus (A). Excitation was at 289 nm, and emission was detected through a 389-nm cut-off filter. The fit shown is to a double-exponential equation with rate constants k_{diss1} and k_{diss2} for the displacement of dansyl-Rab7–REP-1 by Rab7–REP-1 of 0.39 s^{-1} and 0.03 s^{-1}, respectively. (B) Example of fitting rate constants to data of the type shown in (A) by numerical integration (using the program SCIENTIST). The concentrations were 50 nM (dansyl-Rab7–REP-1) and 300 nM (RabGGTase). The values of the fitted rate constants were 5.6×10^7 $M^{-1} \cdot s^{-1}$ for k_{+1} and 5.7 s^{-1} for k_{+2} (Scheme 1).

shown). The first mass corresponds to the calculated molecular mass of Rab7 without the first methionine. The mass of dansyl-Rab7 corresponds to double dansylation and loss of the first methionine. Dansylation was highly efficient as there were only very minor peaks corresponding to undansylated or mono-dansylated protein in the preparation.

On interaction of dansyl-labeled Rab7 with REP-1, there was a large increase in dansyl fluorescence at 440 nm on excitation at 333 nm on titration with REP-1. Titration data could be fitted using a quadratic equation describing the binding curve and were consistent with a 1 : 1 stoichiometry and a K_d value of 600 pM. This K_d value is very close to the one obtained earlier with mantGDP-bound Rab7 [31], suggesting that the presence of the dansyl group did not significantly influence the K_d of the Rab7–REP-1 complex (data not shown). We then tested whether the fluorescent Rab derivative could report on the interaction of RabGGTase with the Rab7–REP-1 complex. When RabGGTase was added to the complex of dansyl-Rab7–REP-1 under the same experimental conditions as above, a further fluorescence increase of nearly 40% was observed (data not shown). There was no observable fluorescence change if RabGGTase was added to dansylated Rab7 in the absence of REP-1, in agreement with the conclusion that only the Rab7–REP-1 complex was recognized by RabGGTase (data not shown). We next titrated 50 nM dansyl-Rab7–REP-1 with RabGGTase. The data obtained were fitted using a quadratic equation (Fig. 3A). A K_d of 13 nM was found which is consistent with a 1 : 1 : 1 stoichiometry.

As the presence of the hydrophobic fluorescence group is likely to have an effect on the interaction of the Rab7–REP-1 complex with RabGGTase, we were interested in determining the affinity of the unmodified complex for RabGGTase. To this end we mixed 50 nM dansyl-Rab7–REP-1 complex with a 10-fold excess of wild-type Rab7–REP-1 complex. The resulting mixture was titrated with RabGGTase. The data obtained were fitted using the program SCIENTIST as described in Experimental Procedures and in the legend to Fig. 3. Keeping the K_d for the fluorescent Rab7–REP-1 constant at the independently determined value of 13 nM, a K_d of 121 nM was obtained for the unmodified complex (Fig. 3B). Thus, the dansylated Rab7–REP-1 complex interacts about 10 times more strongly with RabGGTase than the wild-type.

We next chose to use another label to readdress this potential problem of unspecific interaction of the fluorescent label with RabGGTase, as well as to obtain another estimate of the affinity. To achieve this, we modified C-terminal cysteines with rhodamine using 5-TMRIA as described in Experimental procedures. Labeled protein was analyzed by MS and shown to be over 80% doubly modified. Employing a set of experiments analogous to those performed for dansyl-Rab7 we determined a K_d of 3 nM for the rhodamine-labeled Rab7–REP–1 interaction (data not shown) and a K_d of 140 nM for the rhodamine-labeled Rab7–REP–1 interaction with RabGGTase. From competitive titration experiments, we could extract a K_d of 117 nM for the interaction of the unmodified complex with RabGGTase. This corresponds closely to the value obtained using the dansyl-Rab7-based assay (121 nM) (data not shown).

The affinity of RabGGTase for the Rab7–REP-1 complex was confirmed in an independent manner. We made use of our earlier observation that the Rab7–REP–1 interaction can be monitored via the change in fluorescence of mant derivatives (e.g. mantGDP) bound to Rab7. If the mantGDP–Rab7–REP complex is incubated with a large excess of unlabeled Rab7, a decrease in fluorescence at a rate of about 0.01 s^{-1} can be observed [31]. We performed the same experiment with different amounts of RabGGTase added to the reaction mixture. Addition of transferase slowed the dissociation reaction in a dose-dependent manner. The rates obtained were plotted against the concentration of RabGGTase and fitted with a quadratic equation, yielding a K_d of 172 nM (Fig. 4). This agrees reasonably well with the value derived from the competitive titration experiments.

Transient kinetics of the interaction of dansyl-Rab7–REP-1 with RabGGTase

The fluorescence signal observed on interaction of the dansylated Rab7–REP-1 complex with RabGGTase can also be used for transient kinetic measurements of the interaction, and we have obtained preliminary results. As shown in Fig. 5, mixing of dansyl-Rab7–REP-1 with RabGGTase resulted in a rapid increase in fluorescence when exciting at 295 nm. The curve could be fitted by a double-exponential equation. We repeated the experiment with increasing concentrations of

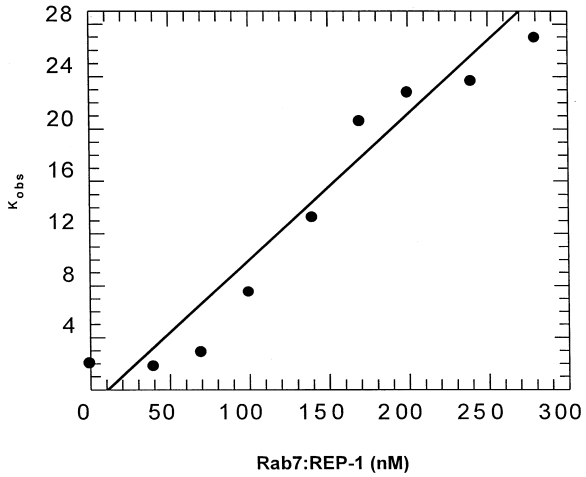

Fig. 7. Secondary plot of the k_{obs} for the rapid phase seen on mixing dansyl-Rab7–REP-1 (10 nM) and wild-type Rab7–REP-1 (40–280 nM) complex with RabGGTase (10 nM) in the stopped-flow apparatus. The reaction conditions and instrument set up were as described for Fig. 6. The k_{+1} for wild-type Rab7–REP-1 obtained from the slope of the plot is 10^8 M^{-1}·s^{-1}.

RabGGTase. From these experiments it appeared that the first phase of the association reaction accelerated as a function of concentration whereas the second phase was noticeably slower and showed only a slight dependence on concentration, which was not easy to characterize because of the relatively inexact determination of the rate constant for the small second phase, but the rate constant for this phase appeared to saturate at ≈ 5 s^{-1}. For the faster phase, there was an approximately linear dependence of the fitted first-order rate constant (Fig. 5). Based on the slope of the straight line obtained from four independent experiments, a value of 4.9×10^7 M^{-1}·s^{-1} was obtained for the association rate constant (k_{ass}). In principle, the dissociation rate constant, k_{off}, can also be estimated from the data. However, this appears to be small, and the important points at lower RabGGTase concentration will not be accurate because pseudo-first-order conditions did not pertain. While this will have little effect on the slope of the fitted line, the intercept is unreliable, so that k_{off} was measured directly in a displacement experiment. Dansyl-Rab7–REP-1–RabGGTase complex (0.1 μM) was mixed with 2 μM unlabeled Rab7–REP-1 complex in the stopped-flow apparatus and the dissociation of dansyl-Rab7–REP-1 was monitored using the FRET signal. The resulting fluorescence trace deviated significantly from a single exponential and was fitted as a double exponential with rate constants of 0.39 s^{-1} and 0.03 s^{-1} (Fig. 6A).

To exclude the possibility that the biphasic kinetic behavior seen was not due to the presence of monolabeled Rab7 in the sample, we used a Rab7 mutant labeled on a single C-terminal cysteine. As for wild-type Rab7, we obtained biphasic binding transients with the kinetic constants 7.1×10^7 M^{-1}·s^{-1} for the concentration-dependent rapid phase and 3.6 s^{-1} for the second phase (data not shown). This indicated that the second phase did not indicate heterogeneity of the dansyl-Rab7 population. The presence of the second phase could not be explained by the residual GGpp bound to RabGGTase. Essentially identical data were obtained if GGpp-free RabGGTase was used in the experiment (data not shown).

The explanation of the existence of two phases in both the association and dissociation kinetics requires further extensive experimentation. At present we conclude that the association process is likely to involve two steps, and a possible model is shown in Scheme 1. The star in the second ternary complex implies that a conformational change has occurred. If we make the assumption that the fluorescence change occurs in the first step, the behavior seen can be explained. Thus, the faster phase would correspond to the initial association reaction, and the second phase would arise from the strengthening of the interaction because of the second step. Taking the slope of the plot of the rate constants of the fast phase against concentration as shown on the inset of Fig. 5 to correspond to k_{+1} in Scheme 1, a value of ≈ 4 s^{-1} for k_{+2} can be derived from individual curves of the time course of interaction of the Rab–REP complex with RabGGTase (see Fig. 6B for an example of fitting rate constants to the data by numerical integration). Scheme 1 does not provide a complete explanation of the kinetic results, as the dissociation kinetics were also markedly biphasic. This cannot be explained on the basis of the two-step scheme with the estimates of the individual rate constants given in Fig. 5, because a phase as slow as the second one in the dissociation reaction as seen in Fig. 6A would not be expected. We therefore conclude that the binding mechanism appears to be complex, with at least two, and possibly three, steps involved, but extensive further studies would be required to establish a definitive model.

$$\text{Rab–Rep} + \text{GGTase} \underset{k_{-1}}{\overset{k_{+1}}{\rightleftharpoons}} \text{Rab–Rep–GGTase} \underset{k_{-2}}{\overset{k_{+2}}{\rightleftharpoons}} \text{Rab–Rep–GGTase*}$$

Scheme 1

In principle, information on the kinetics of interaction of the unmodified Rab7–REP-1 complex with RabGGTase can be obtained by allowing the fluorescently modified and unmodified forms to compete for association with RabGGTase. On increasing the Rab7–REP-1 concentration while keeping the dansyl-Rab7–REP-1 concentration constant and mixing with RabGGTase, a linear increase in the observed rate constant of the fast phase was seen, the slope of which gave a value of $\approx 10^8$ M^{-1}·s^{-1} for the association reaction (Fig. 7). Analysis of the following slower phase was complicated by the uncertainty about the number of steps in the binding reaction, so that a

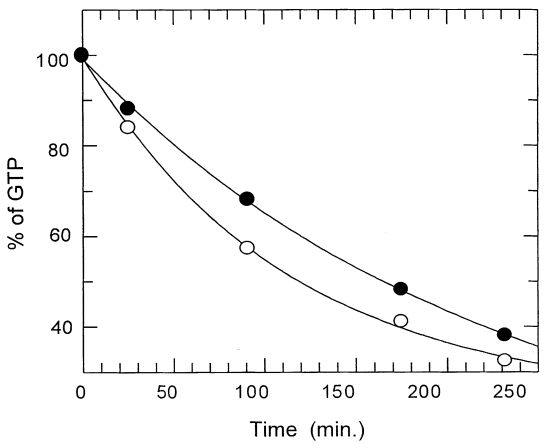

Fig. 8. Effect of RabGGTase on GTP hydrolysis by Rab7. (●) Time course of GTP hydrolysis of a stoichiometric complex of GTP–Rab7–REP-1. (○) Time course when 5 M excess of RabGGTase was added to the sample. The reaction was followed by determining the concentrations of GTP and GDP by HPLC. See Experimental Procedures for a description of the procedure used.

Table 1. Binding affinities of RabGGTase for several mutants of Rab7 in complex with REP-1. Affinities were determined by co-titration with either dansyl-Rab7–REP-1 or rhodamine-labeled Rab7–REP-1. Conditions were as described in Fig. 3. The dansyl-Rab7–REP-1 complex concentration was 50 nM, and that of rhodamine-labeled Rab7–REP-1 was 38 nM.

Mutant	C-Terminal sequence	K_d (nM)
Rab7	EPIKLDKNDRAKTSAESCSC	120
Rab7 C205S	EPIKLDKNDRAKTSAESSSC	193
Rab7 C205S C207S	EPIKLDKNDRAKTSAESSSS	160
Rab7 S206W	EPIKLDKNDRAKTSAESCWC	151
Rab7 ΔC-3	EPIKLDKNDRAKTSAES	233
Rab7 ΔC-3 S204C	EPIKLDKNDRAKTSAEC	209
Rab7 ΔC-16 K191C	EPIC	160
Rab7AlaSer	ESASASASASASASASASAS	264

quantitative analysis was not attempted. It appeared to be due to dissociation of initially bound unlabeled Rab7–REP-1 complex, driven by the higher affinity of the labeled complex. As expected, the overall amplitude of the fluorescence change decreased as the concentration of unlabeled complex was increased. The data obtained, together with the definitive data described above on the relative affinities of labeled and unlabeled complexes to RabGGTase, are consistent with the idea that the initial association reaction proceeds at a similar rate to that of the labeled complex, but that the dissociation rate is significantly faster, in keeping with the lower affinity.

Effect of the nucleotide-bound state of Rab7 on the affinity of RabGGTase for the Rab7–REP-1 complex

Having an assay for interaction of the Rab7–REP-1 complex with RabGGTase in hand, we wanted to determine whether RabGGTase had any preference for the nucleotide-bound state of Rab7. It was shown previously that RabGGTase prenylates Rab proteins preferentially in the GDP-bound form. It was suggested that this difference is mediated by REP-1 preferentially recognizing the GDP-bound form of Rab proteins [33]. To check whether RabGGTase contributes to this discrimination, we repeated the co-titration experiments described above using rhodamine-labeled Rab7 and unlabeled Rab7 preloaded with GppNHp, a non-hydrolyzable analog of GTP. The data were processed as before and gave a K_d value of 121 nM (Fig. 3C). This experiment clearly demonstrates that association of RabGGTase with the Rab7–REP-1 complex is not dependent on the nucleotide-induced conformation of Rab7. A remaining possibility was that RabGGTase can stimulate the rate of GTP hydrolysis, thus converting prenylation-destined Rab proteins into the 'inactive' GDP-bound form. We monitored the influence of REP-1 and/or RabGGTase on the progression of GTP hydrolysis by Rab7 using HPLC. The rates of GDP generation were slightly higher at 5 M excess of RabGGTase over Rab7 at a concentration of 5 μM of the latter (Fig. 8). However, this might be a consequence of some unspecific phosphatase activity in the enzyme preparation because at long incubation times a small GMP peak appeared in samples containing REP-1 or RabGGTase (data not shown) but not when GTP–Rab7 was incubated alone.

Sequence requirements for substrate recognition of RabGGTase

Finally, we addressed the issue of the substrate specificity of RabGGTase. As mentioned in the introduction, the Rab family possesses a diverse array of C-terminal motifs which are all believed to be processed by RabGGTase. One of the possible explanations is that RabGGTase recognizes the C-terminal cysteines directly regardless of the context. Another is that Rab GGTase might recognize some as yet unidentified C-terminal motifs upstream of the two cysteines. It is also imaginable that the transferase recognizes nascent epitopes which form upon Rab7–REP association and then additionally and rather unspecifically interact with the C-terminus of Rab7.

To distinguish between these possibilities, we generated a number of C-terminal mutants of Rab7 (Table 1). Mutants Rab7 C205S and Rab7 C205S C207S contained either only one or no C-terminal cysteines. Mutant Rab7 S206 W contained a bulky group between two prenylatable cysteines. Mutants Rab7 ΔC S204C, Rab7 ΔC and Rab7 ΔC K191C were truncated by 3 and 16 amino acids, respectively, leaving the last residue as either serine or cysteine. Finally the mutant designated Rab7sas has the last 18 amino acids replaced by a repetitive sequence of serine and alanine with serine being the last amino acid. All mutants could form stable complexes with REP-1 as confirmed by analytical gel filtration (data not shown). We then used the competitive titration assays described above to determine the dissociation constants for the interaction of mutant Rab7–REP–1 with RabGGTase. The rhodamine-based and dansyl-based assays produced very similar data. The results obtained are summarized in Table 1. From these data, we conclude that the number of C-terminal cysteines does not significantly influence the affinity of RabGGTase for the Rab–REP complex. The addition of a bulky tryptophan between the C-terminal cysteines also did not affect the binding. Truncation by 3 and 16 amino acids did not lead to a significant decrease in binding affinity. Even the Rab7sas–REP-1 complex interacted with RabGGTase with a K_d value of 264 nM. This demonstrates that the amino acids of the C-terminus make only a limited contribution to the overall affinity of the Rab–REP complex interaction with RabGGTase. Considering the diversity of the C-terminal motifs of Rab proteins and the fact that substitution of cysteine with serine does not lead to a significant decrease in affinity suggests that RabGGTase interacts only weakly with the C-terminus of Rab7, supporting the model that RabGGTase recognizes an epitope or epitopes outside the C-terminus.

DISCUSSION

In the current work, we have explored the interaction of RabGGTase with its protein substrate. Using a gel-filtration assay we showed that RabGGTase forms a stable complex with Rab7–REP-1 in the absence of the lipid substrate GGpp. This is consistent with the findings that GGTase I and farnesyl transferase can form a stable complex with both protein and lipid substrate independently [9,11]. Formation of the stable complex was dependent on the presence of both Rab7 and REP-1, supporting the notion that Rab7 could be recognized by RabGGTase only in its complex with REP-1. Using MS and TLC, we demonstrated that the recombinant RabGGTase purified from the insect cells contained only a very limited amount of GGpp bound to it. We also demonstrated that RabGGTase can be depleted of GGpp by treating the former with alkaline phosphatase.

From the gel-filtration experiments we could conclude that the stoichiometry of the ternary complex was approximately 1 : 1 : 1. In order to measure the affinity of the Rab7–REP–RabGGTase complex formation directly, we developed two

novel assays in which the C-terminal cysteines of Rab7 were labeled with dansyl or rhodamine groups. This approach gave excellent results, perhaps because of large structural rearrangements taking place in the C-terminal region following the association with REP-1 and RabGGTase.

The method allowed accurate determination of K_d values for the dansyl-Rab7–REP-1 and the rhodamine-labeled Rab7–REP-1 interactions with RabGGTase. Taking advantage of the high fluorescent yield and large fluorescence changes, we were able to perform co-titration experiments in which a mixture of wild-type and fluorescently labeled Rab7–REP complex was titrated with RabGGTase. These competition titration experiments enabled us to derive a K_d value of about 120 nM for the unmodified Rab7–REP-1 interaction with RabGGTase. The value obtained for the affinity was confirmed in an independent assay in which we measured the rate of dissociation of the Rab7–REP-1–RabGGTase complex as a function of RabGGTase concentration. This experiment yielded a K_d of 170 nM, which is in satisfactory agreement with that derived from the co-titration experiment.

The original report describing purification of RabGGTase demonstrates that the partially purified RabGGTase activity (including both REP-1 and RabGGTase) was eluted from the gel-filtration column with a retention time corresponding to a molecular mass of 330 kDa [34]. However, the same study indicated that purified RabGGTase migrated at a position corresponding to about 90 kDa. This result might indicate that the ternary complex described above exists as a stable entity *in vivo*. It is conceivable that newly synthesized Rab protein sequentially associates with REP-1 and RabGGTase and then undergoes prenylation when the ternary complex is exposed to GGpp. This model inevitably raises questions about the sequence of protein and lipid substrate binding and the mechanism of double prenylation and substrate release. Elucidation of these problems will require further studies.

We have preliminary evidence that association of RabGGTase with the complex proceeds in a two-step binding mechanism where the first step is fast and concentration-dependent while the second is concentration-independent and rate-limiting at high concentrations. The data obtained indicate K_d values for the interaction with RabGGTase of 13 nM for dansyl-Rab7–REP-1, about 140 nM for rhodamine-labeled Rab7–REP-1 and 120 nM for unmodified Rab7–REP-1. Modification of the C-terminal cysteines with the dansyl groups results in a nearly 10-fold tighter binding of RabGGTase to the Rab7–REP-1 complex. Although we cannot interpret what happens at the molecular level, we speculate that the hydrophobic dansyl group interacts with the putative GGpp-binding pocket of RabGGTase.

Our finding that the affinity of Rab7–REP-1–RabGGTase is high enough to form a stable ternary complex is somewhat at odds with results of other groups which indicated that RabGGTase interacts with Rab–REP complex only transiently and the overall affinity was estimated to be 4 μM [13,35]. The experiments leading to this conclusion were performed under conditions of multiple turnover of the prenylation reaction and therefore do not resolve each individual step of the reaction. We speculate that RabGGTase has a dramatically different affinity for the prenylated and unprenylated Rab–REP-1 complex. This would be consistent with the notion of how the enzyme works and what its biological role in the cell is thought to be and suggests tight binding of the substrate and relatively easy release of the product. As demonstrated in the studies on farnesyl transferase, the lipid and peptide substrate binding can be independent processes [8]. In the case of farnesyl transferase, a binding sequence in which the lipid is bound first seems to be preferred. It would be interesting to know whether the same holds true for RabGGTase, especially considering the difference in the size and nature of the protein substrate. Additional experiments will be necessary to clarify this point.

As we had assays for analyzing the interaction of Rab7–REP-1 with RabGGTase, we chose to re-examine the issue of the nucleotide specificity of RabGGTase. Earlier work established that prenylation of Rab proteins by RabGGTase depends on their nucleotide-bound state, with the GDP-bound state being preferred [33]. This could be attributed at least partially to preferential interaction of REP with GDP-bound conformations of Rab proteins [31,33]. We analyzed whether RabGGTase contributes to this discrimination at the level of substrate binding. No significant difference between the GDP-bound or GppNHp-bound Rab7–REP-1 complexes in their affinity for RabGGTase was detected. This cannot be attributed to the failure of REP-1 to form a complex with Rab7 as the experiments were performed at concentrations at which both nucleotide-bound forms of Rab7 are tightly bound to REP-1 [31]. However, it is yet to be seen whether the different nucleotide-bound conformations confer different behavior in the course of the prenylation reaction or product release. We also tested whether either REP-1 or RabGGTase or a combination of the two could stimulate the GTPase activity of Rab7, and came to a negative conclusion.

Finally, we have presented evidence that RabGGTase recognizes its substrate through interactions with regions other than the C-terminus. By generating a number of mutants, we could demonstrate that neither the cysteines nor the length of the C-terminus are important for substrate recognition of RabGGTase. Even when the last 18 amino acids were replaced by a repetitive Ser–Ala sequence, no dramatic changes in affinity were observed. At least three possible mechanistic models could explain these observations. First, association with REP-1 could induce secondary-structure formation in the otherwise disordered C-terminus of Rab7 and provide a nascent binding site for RabGGTase. However, experiments performed with mutants truncated by as much as 16 amino acids suggest that the C-terminus is not essential for the formation of the ternary complex. Secondly, it is possible that formation of the Rab–REP-1 complex exposes or generates a new epitope recognized by the RabGGTase. In a third model, both REP and Rab would have weaker binding sites for different parts of RabGGTase, and both of these interactions could be simultaneously satisfied in the ternary complex with a consequent dramatic increase in affinity. Our experiments support either the second or the third model. With hindsight, this finding is not surprising, taking into account the diversity of the C-terminal sequence motifs and the variation in length of the C-terminal fragments among Rab proteins. To be active on more then 30 different substrate molecules, RabGGTase must possess a well-developed mechanism for dealing with such structural diversity. One possible mode of action would be that RabGGTase binds to a nascent recognition site arising from interaction of Rab with REP-1, with the flexible C-terminus being positioned in the vicinity of the active center. In the following step, RabGGTase 'scans' the C-terminal tail for available cysteines and prenylates them. However, further extensive experiments will be necessary to delineate the reaction mechanism.

ACKNOWLEDGEMENTS

We thank Heino Prinz for advice and help with mass spectrometry and Milena Kostadinova for help with cell culture and for technical assistance. This work was supported by the Deutsche Forschungsgemeinschaft.

REFERENCES

1. Novick, P. & Zerial, M. (1997) The diversity of Rab proteins in vesicle transport. *Curr. Opin. Cell Biol.* **9**, 496–504.
2. Pfeffer, S.R. (1994) Rab GTPases: master regulators of membrane trafficking. *Curr. Opin. Cell Biol.* **6** , 522–526.
3. Pfeffer, S.R., Dirac-Svejstrup, A.B. & Soldati, T. (1995) Rab GDP dissociation inhibitor: putting rab GTPases in the right place. *J. Biol. Chem.* **270**, 17057–17059.
4. Ullrich, O., Horiuchi, H., Bucci, C. & Zerial, M. (1994) Membrane association of Rab5 mediated by GDP-dissociation inhibitor and accompanied by GDP/GTP exchange. *Nature (London)* **368**, 157–160.
5. Armstrong, S.A., Seabra, M.C., Sudhof, T.C., Goldstein, J.L. & Brown, M.S. (1993) cDNA cloning and expression of the alpha and beta subunits of rat Rab geranylgeranyl transferase. *J. Biol. Chem.* **268**, 12221–12229.
6. Seabra, M.C., Brown, M.S., Slaughter, C.A., Sudhof, T.C. & Goldstein, J.L. (1992) Purification of component A of Rab geranylgeranyl transferase: possible identity with the choroideremia gene product. *Cell* **70**, 1049–1057.
7. Casey, P.J. & Seabra, M.C. (1996) Protein prenyltransferases. *J. Biol. Chem.* **271**, 5289–5292.
8. Pompliano, D.L., Rands, E., Schaber, M.D., Mosser, S.D., Anthony, N.J. & Gibbs, J.B. (1992) Steady-state kinetic mechanism of Ras farnesyl: protein transferase. *Biochemistry* **31**, 3800–3807.
9. Yokoyama, K., McGeady, P. & Gelb, M.H. (1995) Mammalian protein geranylgeranyltransferase-I: substrate specificity, kinetic mechanism, metal requirements, and affinity labeling. *Biochemistry* **34** , 1344–1354.
10. Dolence, J.M., Cassidy, P.B., Mathis, J.R. & Poulter, C.D. (1995) Yeast protein farnesyltransferase: steady-state kinetic studies of substrate binding. *Biochemistry* **34**, 16687–16694.
11. Furfine, E.S., Leban, J.J., Landavazo, A., Moomaw, J.F. & Casey, P.J. (1995) Protein farnesyltransferase: kinetics of farnesyl pyrophosphate binding and product release. *Biochemistry* **34**, 6857–6862.
12. Alexandrov, K., Horiuchi, H., Steele-Mortimer, O., Seabra, M.C. & Zerial, M. (1994) Rab escort protein-1 is a multifunctional protein that accompanies newly prenylated rab proteins to their target membranes. *EMBO J.* **13**, 5262–5273.
13. Shen, F. & Seabra, M.C. (1996) Mechanism of digeranylgeranylation of Rab proteins. Formation of a complex between monogeranylgeranyl-Rab and Rab escort protein. *J. Biol. Chem.* **271**, 3692–3698.
14. Cremers, F.P., Armstrong, S.A., Seabra, M.C., Brown, M.S. & Goldstein, J.L. (1994) REP-2, a Rab escort protein encoded by the choroideremia-like gene. *J. Biol. Chem.* **269**, 2111–2117.
15. Araki, S., Kikuchi, A., Hata, Y., Isomura, M. & Takai, Y. (1990) Regulation of reversible binding of smg p25A, a ras p21-like GTP- binding protein, to synaptic plasma membranes and vesicles by its specific regulatory protein, GDP dissociation inhibitor. *J. Biol. Chem.* **265**, 13007–13015.
16. Brown, M.S. & Goldstein, J.L. (1993) Protein prenylation. Mad bet for Rab. *Nature (London)* **366**, 14–15.
17. Andres, D.A., Seabra, M.C., Brown, M.S., Armstrong, S.A., Smeland, T.E., Cremers, F.P. & Goldstein, J.L. (1993) cDNA cloning of component A of Rab geranylgeranyl transferase and demonstration of its role as a Rab escort protein. *Cell* **73**, 1091–1099.
18. Smeland, T.E., Seabra, M.C., Goldstein, J.L. & Brown, M.S. (1994) Geranylgeranylated Rab proteins terminating in Cys-Ala-Cys, but not Cys-Cys, are carboxyl-methylated by bovine brain membranes in vitro. *Proc. Natl Acad. Sci. USA.* **91**, 10712–10716.
19. Joberty, G., Tavitian, A. & Zahraoui, A. (1993) Isoprenylation of Rab proteins possessing a C-terminal CaaX motif. *FEBS Lett.* **330**, 323–328.
20. Wilson, A.L., Erdman, R.A., Castellano, F. & Maltese, W.A. (1998) Prenylation of Rab8 GTPase by type I and type II geranylgeranyl transferases. *Biochem. J.* **333**, 497–504.
21. Desnoyers, L. & Seabra, M.C. (1998) Single prenyl-binding site on protein prenyl transferases. *Proc. Natl. Acad. Sci. USA* **95**, 12266–12270.
22. Wilson, A.L., Erdman, R.A. & Maltese, W.A. (1996) Association of Rab1B with GDP-dissociation inhibitor (GDI) is required for recycling but not initial membrane targeting of the Rab protein. *J. Biol. Chem.* **271**, 10932–10940.
23. Dirac-Svejstrup, A.B., Soldati, T., Shapiro, A.D. & Pfeffer, S.R. (1994) Rab-GDI presents functional Rab9 to the intracellular transport machinery and contributes selectivity to Rab9 membrane recruitment. *J. Biol. Chem.* **269**, 15427–15430.
24. Anant, J.S., Desnoyers, L., Machius, M., Demeler, B., Hansen, J.C., Westover, K.D., Deisenhofer, J. & Seabra, M.C. (1998) Mechanism of Rab geranylgeranylation: formation of the catalytic ternary complex. *Biochemistry* **37**, 12559–12568.
25. Neu, M., Brachvogel, V., Oschkinat, H., Zerial, M. & Metcalf, P. (1997) Rab7: NMR and kinetics analysis of intact and C-terminal truncated constructs. *Proteins* **27**, 204–209.
26. Parks, T.D., Howard, E.D., Wolpert, T.J., Arp, D.J. & Dougherty, W.G. (1995) Expression and purification of a recombinant tobacco etch virus NIa proteinase: biochemical analyses of the full-length and a naturally occurring truncated proteinase form. *Virology* **210**, 194–201.
27. Simon, I., Zerial, M. & Goody, R.S. (1996) Kinetics of interaction of Rab5 and Rab7 with nucleotides and magnesium ions. *J. Biol. Chem.* **271**, 20470–20478.
28. Armstrong, S.A., Brown, M.S., Goldstein, J.L. & Seabra, M.C. (1995) Preparation of recombinant Rab geranylgeranyltransferase and Rab escort proteins. *Methods Enzymol.* **257**, 30–41.
29. John, J., Sohmen, R., Feuerstein, J., Linke, R., Wittinghofer, A. & Goody, R.S. (1990) Kinetics of interaction of nucleotides with nucleotide-free H- ras p21. *Biochemistry* **29**, 6058–6065.
30. Tucker, J., Sczakiel, G., Feuerstein, J., John, J., Goody, R.S. & Wittinghofer, A. (1986) Expression of p21 proteins in Escherichia coli and stereochemistry of the nucleotide-binding site. *EMBO J.* **5**, 1351–1358.
31. Alexandrov, K., Simon, I., Iakovenko, A., Holz, B., Goody, R.S. & Scheidig, A. (1998) Moderate discrimination of REP-1 between Rab7GDP and Rab7GTP arises from a difference of an order of magnitude in dissociation rate. *FEBS Lett.* **425**, 460–464.
32. Dunten, P., Kammlott, U., Crowther, R., Weber, D., Palermo, R. & Birktoft, J. (1998) Protein farnesyltransferase: structure and implications for substrate binding. *Biochemistry* **37**, 7907–7912.
33. Seabra, M.C. (1996) Nucleotide dependence of Rab geranylgeranylation. Rab escort protein interacts preferentially with GDP-bound Rab. *J. Biol. Chem.* **271**, 14398–14404.
34. Seabra, M.C., Goldstein, J.L., Sudhof, T.C. & Brown, M.S. (1992) Rab geranylgeranyl transferase. A multisubunit enzyme that prenylates GTP-binding proteins terminating in Cys-X-Cys or Cys- Cys. *J. Biol. Chem.* **267**, 14497–14503.
35. Anant, J.S., Desnoyers, L., Burke, S. & Seabra, M.C. (1997) Structure-function studies on Rab escort protein. Abstracts of ECBO 1997 Meeting, Abstract54. Q12

Author Queries

Q1 Please note that the references have been reordered from number **1** onwards

Q2 **Au: Please give BME in full.**

Q3 Au: Please supply company address

Q4 Au: Please supply company city (state), country

Q5 Au: Please supply company city (state), country

Q6 Au: Please supply company city (state), country

Q7 **Au: In Fig. 2B this is 86 kDa. Please check.**

Q8 **Au: Please give names and initials of all workers.**

Q9 **Au: Please give names and initials of all workers.**

Q10 Au: Please supply initials

Q11 **Au: k_{+1} was not actually given on Scheme 1. Are the additions OK?**

Q12 **Au: Any more details available? Publisher? Town of publication? Please give ECBO in full**

Q13 **Au: There is no panel C in Fig 2.**